

Effect of near-field coupling on far-field inelastic scattering imaging of gold nanoparticles

This article has been downloaded from IOPscience. Please scroll down to see the full text article.

2008 Nanotechnology 19 395705

(<http://iopscience.iop.org/0957-4484/19/39/395705>)

[The Table of Contents](#) and [more related content](#) is available

Download details:

IP Address: 155.69.4.4

The article was downloaded on 20/08/2008 at 08:46

Please note that [terms and conditions apply](#).

Effect of near-field coupling on far-field inelastic scattering imaging of gold nanoparticles

YuMeng You, ChaoLing Du, Yun Ma, Johnson Kasim, Ting Yu and ZeXiang Shen¹

Division of Physics and Applied Physics, School of Physical and Mathematical Sciences, Nanyang Technological University, 1 Nanyang Walk, Block 5, Level 3, 637616, Singapore

E-mail: zexiang@ntu.edu.sg


Received 23 May 2008, in final form 10 July 2008

Published 18 August 2008

Online at stacks.iop.org/Nano/19/395705

Abstract

The optical near-field enhancement induced by coupling between noble nanoparticles and the substrate has been studied by a far-field imaging method. The longitudinal mode of the incident laser is revealed to contribute to the coupling. The far-field images of individual gold nanoparticles exhibit a peanut-shaped pattern; these were constructed by the intensity of inelastically scattered light. The coupling between gold nanoparticles and the silicon substrate leads to the patterned image. By tuning the separation between the gold nanoparticles and substrate using SiO₂ layers of different thickness, the coupling efficiency decreases with the thickness of the SiO₂ layer.

 Supplementary data are available from stacks.iop.org/Nano/19/395705

(Some figures in this article are in colour only in the electronic version)

1. Introduction

Noble metal nanoparticles have attracted much attention since the 19th century. In the last decade, investigation of surface plasmons has revived intense interest in noble metal nanoparticles, which have found wide application in surface enhanced Raman spectroscopy (SERS) [1, 2], plasmonic crystals [3], biosensors [4] and nanolithography [5]. Surface plasmons can be excited on noble metal nanoparticles and localized in very small volumes of metal nanoparticles. Such highly confined electric fields can enhance inelastic scattering of light as Raman and photoluminescence (PL) [6, 7] signals. When a very sharp metal tip with a diameter around 10–100 nm is used, the spatial resolution and intensity of Raman imaging can be impressively improved [8–11] due to the ‘lightning rod’ or ‘antenna’ effect [12]. Different aspects of localized surface plasmons excited on noble metal nanoparticles have also been theoretically studied, such as particle sizes, shapes, assembly structures and their physical environment [13–18]. Since a substrate is normally necessary to support metal nanostructures in real experiments, one needs to consider the

interaction between metal nanostructures and the supporting substrate—known as the substrate effect [19, 20] or ‘gap mode’ effect [21]. Careful selection of substrates allows the local electromagnetic field to be greatly enhanced. Even more importantly, the lateral resolution can be improved to less than 1 nm even with a relatively large tip (20 nm), leading to molecular-scale spatial resolution [22, 23]. However, until now, most of the experiments concerning substrate effects of individual nanostructures have been carried out in the near-field. Although such near-field techniques can provide a much better spatial resolution, the introduced sharp tip affects the local field distribution near the metal nanoparticles. Here, we perform far-field inelastic scattering (IS) imaging to study the near-field ‘gap mode’ effect of metal nanoparticles on different thicknesses of SiO₂ on silicon substrates.

2. Experimental details

In our experiments, imaging of inelastically scattered light (ISL) was carried out on gold nanoparticles in the far-field by a WiTec CRM200 Raman system with a 100× objective lens (numerical aperture (NA) 0.95). The samples were

¹ Author to whom any correspondence should be addressed.

scanned by a piezo-stage with step size smaller than 10 nm and the excitation source was a 532 nm Nd:YAG laser. In the imaging process, the spectra were collected while scanning the sample with a step size of 50 nm. Then the computer analyzed the data and constructed the images from the intensity of the ISL. Different thicknesses of SiO₂ were grown on silicon by annealing (for thicknesses less than 50 nm) and pulsed laser deposition (for 6 nm and 100 nm thicknesses). The growth condition of SiO₂ can be found in supporting information (available at stacks.iop.org/Nano/19/395705). A diluted colloidal solution of gold nanoparticles (diameter 50 ± 5 nm, Corpuscular Inc.) was dispersed on the SiO₂/Si substrates and dried at room temperature. A scanning electron microscope (SEM) (Jeol JSM-6700F) was used to study the shape of the nanoparticles and locate the positions of the individual nanoparticles. The simulation was performed by a finite element method (FEM) in COMSOL MULTIPHYSICS.

3. Results and discussion

Figure 1(a) shows a SEM image of gold nanoparticles on a silicon substrate with a SiO₂ thickness around 6 nm. The inter-particle distance among the Au particles was large enough (more than 1 μm) for the coupling between nanoparticles to be neglected [24]. Figure 1(b) is an ISL image of the area indicated by the red square in figure 1(a), and the contrast of the image indicates the integrated intensity of ISL collected from gold nanoparticles in the range of 550–600 nm. It can be seen that the positions of gold nanoparticles in ISL imaging correspond very well with those shown in the SEM image. The blue circles are a guide for the eyes of the positions of gold nanoparticles. Several gold nanoparticles can be found in the SEM image, and we focus on the single nanoparticles, as indicated by the purple arrow in figure 1(a). The ISL imaging

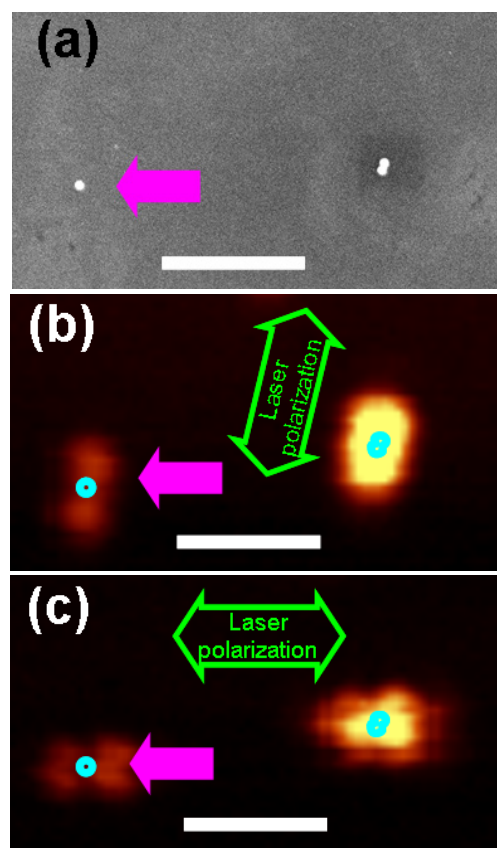


Figure 1. (a) SEM image of gold nanoparticles on a silicon substrate with a 6 nm SiO₂ 'gap'. (b), (c) ISL images taken at the same location shown as (a), with incident laser of horizontal polarization (b) and vertical polarization (c). The purple arrows indicate a single gold nanoparticle. Blue circles in (b) and (c) are guides to the eyes to indicate the positions of gold nanoparticles. Green arrows show the polarization direction of the incident laser. The white scale bar is 1 μm .

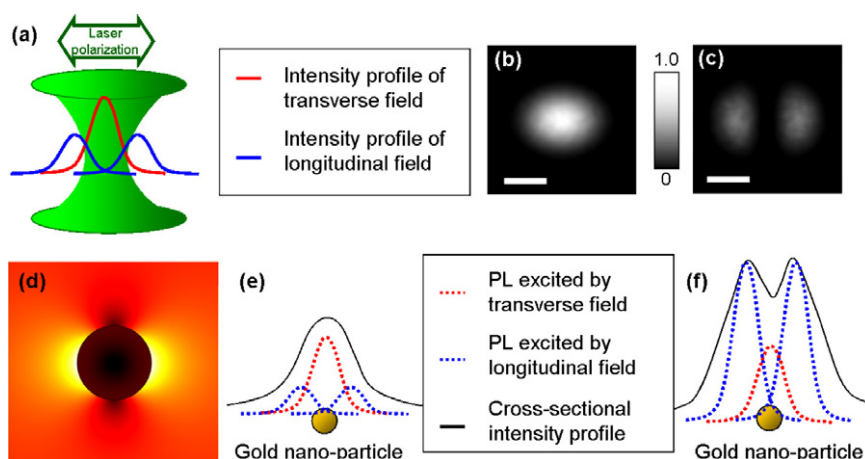


Figure 2. (a) Schematic diagram showing the distribution of the incident laser field. The normalized intensity of the calculated field distribution of the incident laser at the focal plane is plotted for the TM field (b) and for the LM field (c). (d) The calculated field distribution of a 50 nm diameter spherical gold nanoparticle. The nanoparticle is illuminated by a uniform incident field of 532 nm laser light with horizontal polarization (hence it is a TM field only). The cross-sectional ISL intensity profiles under weak and strong nanoparticle–substrate coupling conditions are shown in (e) and (f), respectively. The intensity of ISL excited by the LM field is stronger in (f) because of the strong coupling. Hence the splitting looks more obvious.

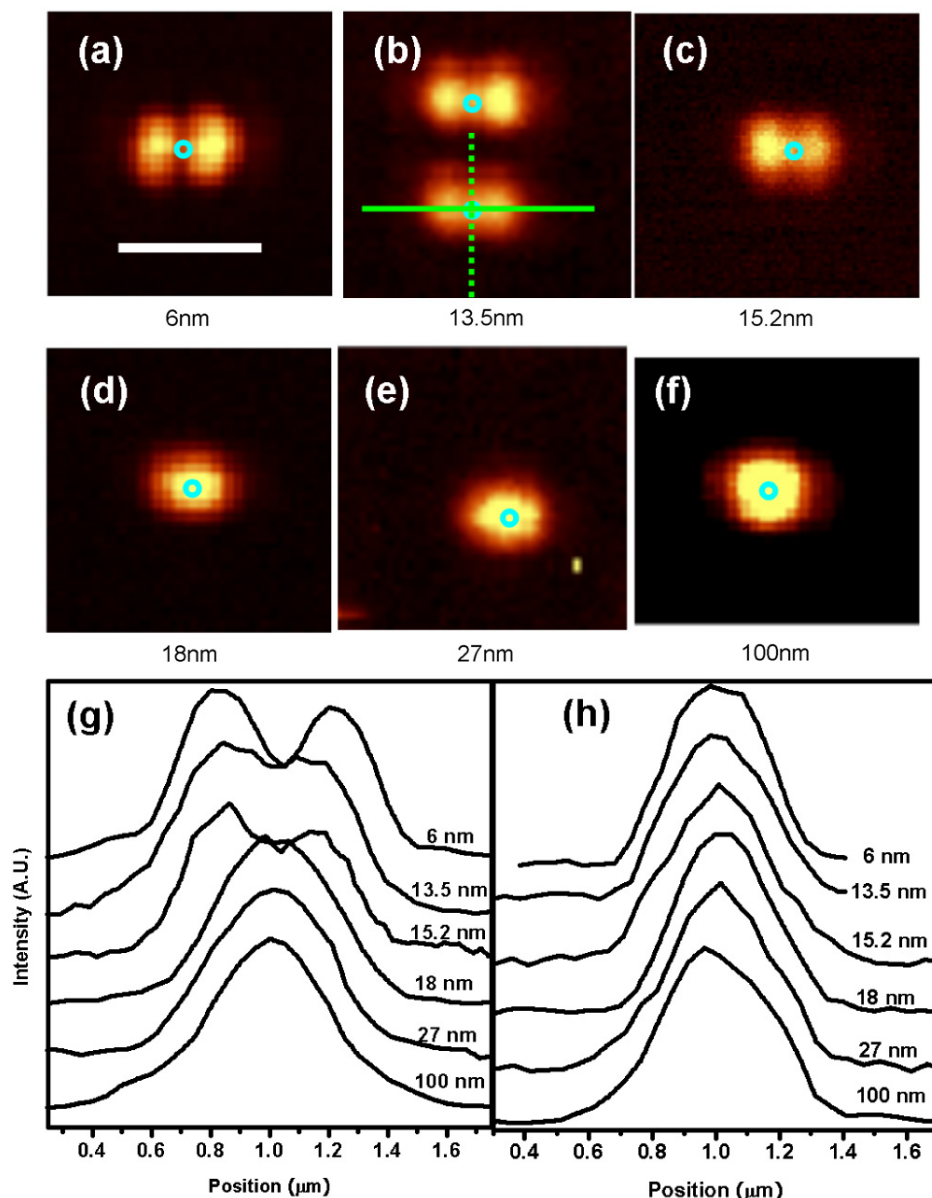


Figure 3. (a)–(f) ISL imaging results from individual gold nanoparticles on substrates with different SiO₂ thicknesses. The imaging area for (a)–(f) is $2\ \mu\text{m} \times 2\ \mu\text{m}$ and the scale bar in part (a) is $1\ \mu\text{m}$. In (a)–(f) the direction of laser polarization is always horizontal. (g), (h) Comparison of cross-sectional ISL intensity profile (g) along the direction of laser polarization and (h) perpendicular to the direction of laser polarization.

results are shown in figures 1(b) and (c). The ISL images show peanut-shaped patterns with two maximum intensity spots located at the sides of the nanoparticle, and the distance between the two spots is about $350\ \text{nm}$. This ISL intensity distribution shows strong polarization dependence. By rotating the polarization of incident laser, the distribution pattern of ISL intensity also rotates correspondingly, as shown in figure 1(c).

Normally, at the focus point the incident laser can be approximated as a plane wave with Gaussian distribution, called the transverse mode (TM) of the laser. The polarization direction of the TM field is parallel to the sample surface and perpendicular to the direction of propagation of the laser. When excited by such a TM field, the most intense field is found at the two poles of the nanoparticle along the polarization direction of the exciting electric field [25],

as illustrated in figure 2(d). However, due to our far-field experimental setup, these two intense spots on the particle surface are too close ($50\ \text{nm}$, equal to the diameter of nanoparticle) to be resolved. Hence the peanut-shaped ISL pattern of a single gold nanoparticle in figure 1(b) is not caused by the TM field of the incident laser. It is well known that by using a high NA objective lens, a strong longitudinal mode (LM) field can be created near the focal point [26], as illustrated by figure 2(a). Figures 2(b) and (c) show the calculated spatial intensity distribution of the TM and LM field in the focal plane of a tightly focused Gaussian beam with a NA of 0.95. In figure 2(c), two bright lobes of equal intensity and oriented along the direction of polarization of the beam can be seen. The direction of such a LM field is parallel to the direction of propagation of the beam and localized at the sides

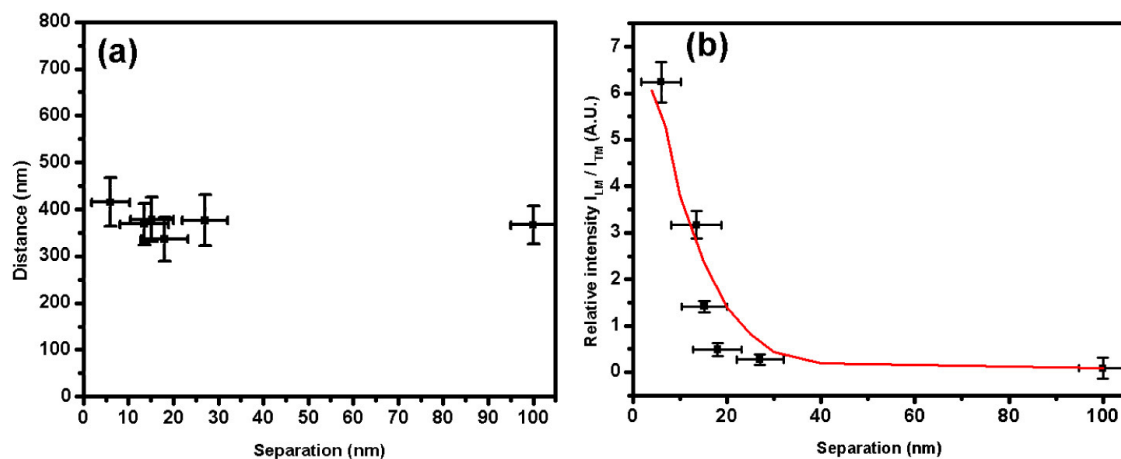


Figure 4. (a) Distance between the two ISL peaks induced by the LM field. (b) Relative intensity I_{LM}/I_{TM} of PL induced by the LM field as a function of nanoparticle–substrate separation.

of the focal point. The LM field spatial distribution pattern in figure 2(c) matches well with our experimental results, not only in the shape and polarization dependence but also the separation between the two lobes. We therefore conclude that the peanut-shaped pattern in our ISL imaging is due to the presence of the LM field of our tightly focused laser beam.

When a focused laser spot was scanned across gold nanoparticles, ISL was excited by both the TM field and the LM field. The spatial distribution of ISL intensity should reflect the intensity distribution of the laser spot shown in figure 2(a). Thus both TM and LM components contribute to the cross-sectional intensity profile of gold nanoparticle ISL, as shown in figures 2(e) and (f). The middle peak is due to the TM component, located at the exact position of nanoparticle, and the other two peaks are excited by the LM component, located at the sides of the nanoparticle oriented along the direction of polarization of the incident light. Normally, the LM field is weaker than the TM field, leading to an intensity distribution profile seen in figure 2(e). The two peaks at the sides are not very obvious compared to the middle peak, so that the weak LM field induced ISL peaks merged with those of the TM field. But in our case the intensity of the LM field induced peaks is much higher than those of the TM field, causing the splitting pattern illustrated in figure 2(f). We attribute the ISL enhancement induced by the LM field to the strong coupling between the silicon substrate and the gold nanoparticle, in agreement with theoretical studies [27–29]. In the ‘gap mode’ model, a gold nanoparticle with a diameter of about 50 nm can be approximated to be an electric dipole polarized by the incident laser. When the distance between gold nanoparticles and the silicon substrate is small enough, the dipole of the gold nanoparticle and its imaginary dipole inside the substrate can couple and cause steep enhancement of local electric field, and generate a much stronger ISL from gold nanoparticles [30].

To further study the substrate effect, we spread the gold nanoparticles on different thicknesses of SiO₂ on silicon substrates and performed similar ISL imaging measurements. The different SiO₂ thickness in these samples serves as a medium for adjusting the distance between gold nanoparticles

and their imaginary dipole. The results are shown in figure 3. Figures 3(a)–(f) are the ISL images of samples with different SiO₂ thicknesses of about 6 nm, 13 nm, 15 nm, 18 nm, 27 nm and 100 nm, respectively. The blue circles are guides to locate the positions of the gold nanoparticles. When the gold nanoparticles are immobilized on the substrate with a 100 nm SiO₂ separation, the most intense point of the ISL pattern (figure 3(f)) is sitting on the exact position of the ISL pattern and appears as an elliptical shape. The intensity pattern splits as the SiO₂ separation decreases. Finally, the ISL intensity distribution pattern becomes two bright lobes at the sides of the gold nanoparticles, as shown in figure 3(a). Figure 3(g) compares the cross-sectional ISL intensity profiles of single gold nanoparticles along the direction of laser polarization as indicated by the green solid line in figure 3(b). From those images we can conclude that while decreasing the separation between nanoparticles and silicon the coupling efficiency between them becomes promoted as well. Larger coupling will excite a stronger ISL from gold nanoparticles, which makes the splitting more obvious. The cross-sectional ISL intensity profiles of the same nanoparticles taken perpendicular to the direction of laser polarization are shown in figure 3(h). No obvious change is found in figure 3(h) for different SiO₂ thicknesses, because the laser LM field only exists along the direction of laser polarization.

To quantify the coupling relationship, the cross-sectional ISL intensity profiles of different samples were then fitted by three peaks (two from the LM induced component and one from the TM induced component), and the results are shown in figure 4. Figure 4(a) plots the separation between two ISL peaks excited by the TM field as a function of the SiO₂ ‘gap’ thickness. The separation remains approximately constant (between 300 and 400 nm). Firstly, this is to be expected as such separation is caused by the non-uniformity of incident laser at the focal plane but not the thickness of SiO₂. Secondly, the separation is equal to the distance between the two maximum incident LM fields at the focal plane, which is a constant in our experiment setup. On the other hand, the

intensity of LM induced ISL is very sensitive to the distance between the nanoparticle and the silicon surface, because such coupling is characteristic of the near-field. Figure 4(b) plots the relative ISL intensity (I_{LM}/I_{TM}) as a function of gold nanoparticles–silicon substrate separation. The data points fit well with simulation results. From the data we can see that the coupling of gold nanoparticles and silicon becomes less effective when the separation is greater than 20 nm, which agrees with the evanescent behavior of this near-field phenomenon. The experimental curve shows a good similarity to the literature where an AFM tip with a gold coating or gold nanoparticles is used [30, 31].

4. Conclusion

In this paper we report the observation of near-field coupling between gold nanoparticles and a silicon substrate by far-field imaging. The coupling-induced peanut-shaped pattern of the ISL intensity distribution is also studied. Our results show that the coupling between gold nanoparticles and silicon substrate can enhance the ISL. By introducing different thicknesses of SiO₂ layers between a silicon substrate and gold nanoparticles, the enhancement can be controllably varied. Such an effect can also be used to carry out SERS by attaching the molecule between gold nanoparticles and a substrate, and may also apply to nanolithographic technology. Further SERS experiments are under way.

References

- [1] Dornhaus R, Benner R E, Chang R K and Chabay I 1980 Surface-plasmon contribution to Sers *Surf. Sci.* **101** 367–73
- [2] GarciaVidal F J and Pendry J B 1996 Collective theory for surface enhanced Raman scattering *Phys. Rev. Lett.* **77** 1163–6
- [3] Grigorenko A N, Geim A K, Gleeson H F, Zhang Y, Firsov A A, Khrushchev I Y and Petrovic J 2005 Nanofabricated media with negative permeability at visible frequencies *Nature* **438** 335–8
- [4] Haes A J and Van Duyne R P 2002 A nanoscale optical biosensor: sensitivity and selectivity of an approach based on the localized surface plasmon resonance spectroscopy of triangular silver nanoparticles *J. Am. Chem. Soc.* **124** 10596–604
- [5] Heltzel A, Theppakuttai S, Chen S C and Howell J R 2008 Surface plasmon-based nanopatterning assisted by gold nanospheres *Nanotechnology* **19** 025305
- [6] Okamoto K, Niki I, Shvartser A, Narukawa Y, Mukai T and Scherer A 2004 Surface-plasmon-enhanced light emitters based on InGaN quantum wells *Nat. Mater.* **3** 601–5
- [7] Kuhn S, Hakanson U, Rogobete L and Sandoghdar V 2006 Enhancement of single-molecule fluorescence using a gold nanoparticle as an optical nanoantenna *Phys. Rev. Lett.* **97** 017402
- [8] Hayazawa N, Inouye Y, Sekkat Z and Kawata S 2001 Near-field Raman scattering enhanced by a metallized tip *Chem. Phys. Lett.* **335** 369–74
- [9] Anderson M S 2000 Locally enhanced Raman spectroscopy with an atomic force microscope *Appl. Phys. Lett.* **76** 3130–2
- [10] Stockle R M, Suh Y D, Deckert V and Zenobi R 2000 Nanoscale chemical analysis by tip-enhanced Raman spectroscopy *Chem. Phys. Lett.* **318** 131–6
- [11] Bar G, Rubin S, Cutts R W, Taylor T N and Zawodzinski T A 1996 Dendrimer-modified silicon oxide surfaces as platforms for the deposition of gold and silver colloid monolayers: preparation method, characterization, and correlation between microstructure and optical properties *Langmuir* **12** 1172–9
- [12] Patane S, Gucciardi P G, Labardi M and Allegrini M 2004 Apertureless near-field optical microscopy *Rev. Nuovo Cimento* **27** 1–46
- [13] Jain P K, Lee K S, El-Sayed I H and El-Sayed M A 2006 Calculated absorption and scattering properties of gold nanoparticles of different size, shape, and composition: applications in biological imaging and biomedicine *J. Phys. Chem. B* **110** 7238–48
- [14] Govorov A O, Bryant G W, Zhang W, Skeini T, Lee J, Kotov N A, Slocik J M and Naik R R 2006 Exciton–plasmon interaction and hybrid excitons in semiconductor–metal nanoparticle assemblies *Nano Lett.* **6** 984–94
- [15] Schatz G C 2001 Electrodynamics of nonspherical noble metal nanoparticles and nanoparticle aggregates *J. Mol. Struct. Theochem.* **573** 73–80
- [16] Jensen T, Kelly L, Lazarides A and Schatz G C 1999 Electrodynamics of noble metal nanoparticles and nanoparticle clusters *J. Clust. Sci.* **10** 295–317
- [17] Mock J J, Barbic M, Smith D R, Schultz D A and Schultz S 2002 Shape effects in plasmon resonance of individual colloidal silver nanoparticles *J. Chem. Phys.* **116** 6755–9
- [18] Noguez C 2007 Surface plasmons on metal nanoparticles: the influence of shape and physical environment *J. Phys. Chem. C* **111** 3806–19
- [19] Wind M M, Bobbert P A, Vliieger J and Bedeaux D 1987 The polarizability of a truncated sphere on a substrate-2 *Physica A* **143** 164–82
- [20] Wind M M, Vliieger J and Bedeaux D 1987 The polarizability of a truncated sphere on a substrate—I *Physica A* **141** 33–57
- [21] Hayashi S 2001 *Near-Field Optics and Surface Plasmon Polaritons* (Berlin: Springer) pp 71–95
- [22] Downes A, Salter D and Elflick A 2006 Finite element simulations of tip-enhanced Raman and fluorescence spectroscopy *J. Phys. Chem. B* **110** 6692–8
- [23] Notingher I and Elflick A 2005 Effect of sample and substrate electric properties on the electric field enhancement at the apex of SPM nanotips *J. Phys. Chem. B* **109** 15699–706
- [24] Su K H, Wei Q H, Zhang X, Mock J J, Smith D R and Schultz S 2003 Interparticle coupling effects on plasmon resonances of nanogold particles *Nano Lett.* **3** 1087–90
- [25] Okamoto H and Imura K 2006 Near-field imaging of optical field and plasmon wavefunctions in metal nanoparticles *J. Mater. Chem.* **16** 3920–8
- [26] Bouhelier A, Beversluis M R and Novotny L 2003 Near-field scattering of longitudinal fields *Appl. Phys. Lett.* **82** 4596–8
- [27] Novotny L, Sanchez E J and Xie X S 1998 Near-field optical imaging using metal tips illuminated by higher-order Hermite–Gaussian beams *Ultramicroscopy* **71** 21–9
- [28] Gozhenko V V, Grechko L G and Whites K W 2003 Electrodynamics of spatial clusters of spheres: substrate effects *Phys. Rev. B* **68** 125422
- [29] Lazzari R, Simonsen I, Bedeaux D, Vliieger J and Jupille J 2001 Polarizability of truncated spheroidal particles supported by a substrate: model and applications *EurPhys. J. B* **24** 267–84
- [30] Knoll B and Keilmann F 2000 Enhanced dielectric contrast in scattering-type scanning near-field optical microscopy *Opt. Commun.* **182** 321–8
- [31] Kim Z H and Leone S R 2006 High-resolution apertureless near-field optical imaging using gold nanosphere probes *J. Phys. Chem. B* **110** 19804–9